

RECENT PROGRESS OF RESEARCH AND DEVELOPMENT FOR THE COST-EFFECTIVE, ENERGY-EFFICIENT PROTON ACCELERATOR CYCIAE-2000*

Tianjue Zhang[†], Wei Fu, Chuan Wang, Shilun Pei, Zhiguo Yin, Hongji Zhou, Ziyue Yin, Hao Le, Suping Zhang, Jingyuan Liu, Xiaofeng Zhu, Fei Wang, Yang Wang, Hongru Cai, Gaofeng Pan, Xianlu Jia, Zhaojun Jin, Xueer Mu, Jun Lin, Bohan Zhao, Aolai He, Zhichao Chu, Mingzhi Hu, Qiqi Song, and the Cyclotron Team at CIAE
China Institute of Atomic Energy, Beijing 102413, P R China

Abstract

The MW class proton accelerators are expected to play important roles in many fields, attracting institutions to continue research and tackle key problems. The continuous wave (CW) isochronous accelerator obtains a high-power beam with higher energy efficiency, which is very attractive to many applications. Scholars generally believe that the energy limitation of the isochronous cyclotron is ~ 1 GeV. Enhancing the beam focusing becomes the most crucial issue for the isochronous machine to get higher beam power.

Adjusting the radial gradient of the average magnetic field makes the field distribution match the isochronism. When we adjust the radial gradient of the peak field, the first-order gradient is equivalent to the quadrupole field, the second-order, the hexapole field, and so on. Just like the synchrotron, there are quadrupoles, hexapole magnets, and so on, along the orbits to get higher energy, as all we know.

If we adjust the radial gradient for the peak field of an FFA's FDF lattice and cooperate with the angular width (azimuth flutter) and spiral angle (edge focusing) of the traditional cyclotron pole, we can manipulate the working path in the tune diagram very flexibly. During enhancing the axial focusing, both the beam intensity and the energy of the isochronous accelerator are significantly increased. And a 2 GeV CW FFA with 3 mA of average beam intensity is designed. It is essentially an isochronous cyclotron, although we use 10 folders of FDF lattices. The key difficulty is that the magnetic field and each order of gradient should be accurately adjusted in a large radius range.

As a high-power proton accelerator with high energy efficiency, we adopt high-temperature superconducting (HTS) technology for the magnets. 15 RF cavities with a Q value of 90000 provide energy gain per turn of ~ 15 MeV to ensure the CW beam intensity reaches 3 mA. A 1:4 scale, 15-ton HTS magnet, and a 1:4 scale, 177 MHz cavity, have been completed. The results of such R&D will also be presented in this paper.

INTRODUCTION

High energy and high current proton accelerators are widely and importantly applied in frontier research fields

* This work was supported in part by the National Natural Science Foundation of China under Grant 12135020 and the basic research fund from the Ministry of Finance of China under Grant BRF201901.

[†] 13641305756@139.com

such as nuclear physics and particle physics, national economic fields such as public health and advanced energy, and even national security [1, 2]. A Proton accelerator with an average beam power of 5-10 MW has been the world's dream machine for more than 30 years [3, 4]. LINAC is considered to be the most promising, and high-energy CW superconducting LINAC is still under development so far [5]. On the other hand, a serious limitation of CW cyclotrons is the maximum energy achievable, which for protons is about 1 GeV for isochronous operation, due to relativistic effects [6, 7]. A 2 GeV CW FFA (or it can be called an alternating gradient cyclotron) has been investigated since 2013 at CIAE, and more detailed R&D activities have been conducted in recent years. The design goal is to provide a 6 MW proton beam with higher energy efficiency than LINAC. It is expected to be up to 30% with overall energy efficiency and keep the cyclotron's advantages of being cost effective for construction and operation.

GENERAL CONSIDERATIONS IN THE OVERALL DESIGN OF 2 GEV CW FFA

Basic Description and Progress of Overall Design since 2019

The 2 GeV FFA facility, CYCIAE-2000, consists of three stages: a 100 MeV isochronous cyclotron as a pre-injector, an 800 MeV isochronous cyclotron as an injector, and the main machine of 2 GeV CW FFA, which are shown in Fig. 1. Compared with the design scheme published in 2019, the main progress is summarized as follows.

FDF field distribution In the previous study [8], the working path in the tune diagram which crosses the resonance of $\nu_r=3$ asks to control the third harmonics B3 at about 1 Gs level. This is particularly challenging for magnet construction. Two more possible solutions to the working path were studied and will be described in the following sections of this paper. Instead of the tremendous amount of tentative numerical calculations by adjusting the magnetic field intensity, angular width, and spiral angle of the 10-fold F and D magnets, along the radius, the third-order peak field distribution of F and D magnets, was analysed into zero-order (dipole, traditional cyclotron sector field), first-order (quadrupole), second-order (hexapole), and third-order (octupole) radial gradients of the peak magnetic field. This method of accurately adjusting the radial gradients of the peak magnetic field, assisted by traditional

edge focusing means, makes it easier, more flexible, and more convenient to build the required working path in the tune diagram.

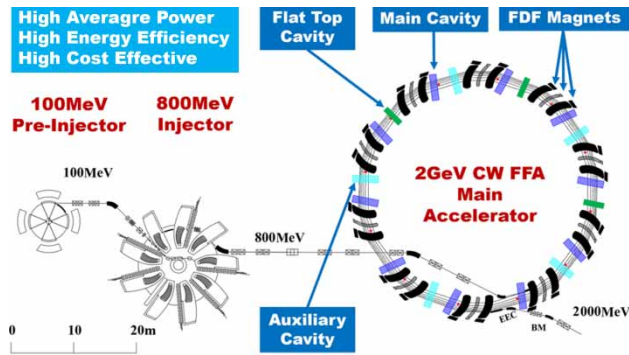


Figure 1: Layout of 2 GeV CW FFA accelerator complex.

Several issues of injection, extraction, current limitation and related RF in the overall design Compared with the 2019 design, the injection from the 800 MeV cyclotron into the 2 GeV main machine is also improved, as shown in Fig. 1. Based on the preliminarily matching by TRACE3D, except the longitudinal matching of the bunch and the buncher design. The extractions by various methods are also investigated. Considering that turn separation is the rigid demand for high current beam extraction, five RF cavities are added to the original design of 10 RF cavities so that the energy gain per turn is up to 15 MeV. Thereby, the turn separation is increased from 10 mm to 15 mm, and the turn separation can be further increased to about 30 mm by precession. This is also conducive to ensuring a high intensity of the circulating beam. From the PSI's experience, the beam intensity, dominated by the space charge, is proportional to the third power of the energy gain per turn [9]. The current limit of this 2 GeV machine can also be estimated by using the method proposed by Dr. Baartman in 2013 for separated turn cyclotrons [10]:

$$I_{max} = \frac{h}{2g_r \xi^3 \beta^3 \gamma v_x^4} \frac{V_{rf}^3}{V_m^2 Z_0} \approx 5.3 \text{ mA} \quad (1)$$

The beam intensity of ~5 mA for 10 MeV and more than 10 mA for 15 MeV energy gain per turn. Such a high current limitation is also due to the big transverse acceptance of FFA. It is conservatively estimated to be 3 mA/6 MW for this overall design. It can be seen that the design will enable the 2 GeV FFA machine to have a potential to hit the ultimate aim of 10 MW average beam power.

In this configuration, we still have five valleys with enough space, one for injection/extraction and the rest for flattop cavities. The multi-particle simulation shows that the flattop cavities can effectively reduce the radial size of the bunch. In case of the worst case, the expectation of this high-power machine operation is assuming two RF systems fail. Our solution is to improve the Q value of each main RF cavity in the design stage. Then we should be able to increase the acceleration voltage of each RF cavity by 20% to maintain the 15 MeV energy gain per turn. At present, we have completed the 1:4 scale RF cavity test, and the test result of the Q value encourages this idea.

The vertical tune shift for space charge dominated beam is well-known [11] and can be derived into a more convenient form for isochronous cyclotrons [12]:

$$\Delta(\nu_z^2) = -\frac{4}{\beta\gamma^3} \cdot \frac{I}{I_0} \cdot \frac{R_\infty}{b(a+b)} \quad (2)$$

Taking into account the relativistic effects of the high energy beam, γ^3 has been added to the denominator. The tune shift results of the space charge effect for 3 mA and 6 mA CW beams, respectively, are shown in Fig. 2. It should be clarified that the vertical tune in Fig. 2 is different from the one we proposed in 2019 and the radial tune avoids the $\nu_r=3$ resonance. For the 6 mA beam, we can find that the tune shift by space charge is 0.1 in 800 MeV and 0.025 near the extraction region specifically. It demonstrates again that the 3 mA/6 MW is a confident design.

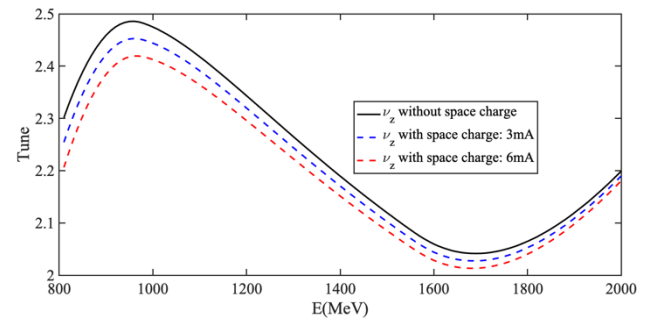


Figure 2: The vertical tune shift of 3 mA and 6 mA CW beams.

The Fermilab researcher reported the energy efficiencies of the three operational accelerators with the highest beam power in the world [13]. The energy efficiency of the PSI isochronous cyclotron is about 3 times of the other types. The isochronous accelerator is an excellent technical route to develop high average beam power, high power efficiency, and high cost-effective proton machine. It can be estimated optimistically that the energy efficiency of a 2 GeV CW FFA with 3 mA of average beam intensity can be increased from PSI's ~20% to 30% if a high-temperature superconducting magnet is used to replace the room temperature magnet at PSI, and an RF cavity with a Q value of 90000 to replace the 45000 cavities at PSI. 1:4 scale equipment: high-temperature superconducting magnet based on YBCO tape and high Q RF cavity have been processed and measured to verify the feasibility of the design, which will also be presented in this paper.

Realization Strong Focusing with Adjustment of Magnetic Field Gradients in Wide Radial Range

Synchrotrons work by rapidly and synchronously adjusting the RF frequency and the magnetic field to match the relativistic effect of the accelerated beam. In a synchrotron, the particle orbits are fixed within a small radial range, and the tune is easily controlled so that the energy can reach higher levels than in a cyclotron. It is comfortable to arrange quadrupole, hexapole, and octupole magnets along the orbit, obtain strong focusing, adjust the working path

in the tune diagram flexibly, traverse various resonances, and get a high energy acceleration ultimately.

Besides the bending effect, the main magnets of CYCIAE-2000 provides an additional focusing effect by adjusting the radial gradient, which is equivalent to the quadrupole, hexapole, and octupole magnets particularly used in the synchrotron. Introducing the first-order, second-order, and third-order gradients of the peak magnetic field in a wide radial range provides strong focusing and an approach to realizing chromaticity compensation. Most importantly, modulating the magnetic field gradient in a wide radial range provides a means to modulate the tune diagram flexibly during acceleration. In CYCIAE-2000, the FDF lattice design was adopted. Each focusing and defocusing magnet has a third-order magnetic field gradient in the radial direction, which can achieve the effect of the dipole to octupole magnets, and thereby balance the isochronism and focusing. Based on this principle of adjusting gradient to provide strong focusing, we add higher-order nonlinear magnetic field components, e.g. quadrupole, hexapole, octupole, etc., at important resonance crossing, resulting in a "radial local achromatic" effect.

BEAM DYNAMICS

Resonance Study

As mentioned above, we have completed a scheme to avoid integer resonance using regulation of radial peak field, which is numbered as Scheme 2. The tune diagram which contains three possible working paths is illustrated in Fig. 3.

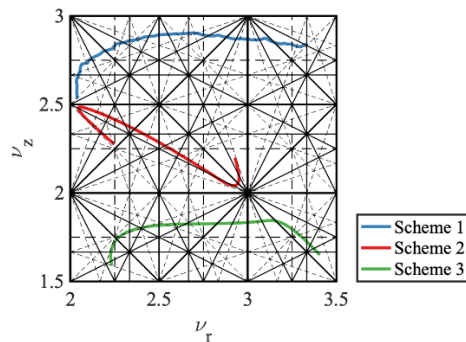


Figure 3: Tune diagram.

Resonance study is carried out especially for Scheme 2. We have summarized the crossed resonance lines for the three schemes in the Table I. This table shows that low-order resonances, such as integer resonances, are the main barriers for higher energy acceleration, especially for the CW FFA machine. Part of the numerical simulation results can be found in Ref [14]. It can be concluded that with the benefit of a strong focusing of the alternating radial gradient, the axial envelope is effectively controlled for the coupled resonances. In summary, also through the multi-particle simulation, the beam envelope does not significantly increase when considering the non-ideal magnetic field, except for the second harmonic field at some particular phases. These simulations show that the lattice structure design of Scheme 2 can tolerate a certain amount of non-

ideal magnetic field components and is feasible in magnet construction.

Table 1: Summary of resonance study

Resonance	Driving term	Scheme 1 Energy	Scheme 2 Energy	Scheme 3 Energy
$\nu_r = 2$	B_2	800~850	800~900	/
$\nu_r = 3$	B_3	1640~1680	1850~2000	1690
$2\nu_r = 5$	dB_5/dr	1280	1280	1320
$\nu_r - \nu_z = 0$	$d\bar{B}/dr$	1560	1120	/
$\nu_r + \nu_z = 5$	dB_5/dr	1030	1640	1870
$\nu_r + 2\nu_z = 7$	d^2B_7/dr^2	/	1390	/
$\nu_r - 2\nu_z = -2$	d^2B_2/dr^2	/	1250	/
$2\nu_r - \nu_z = 2$	d^2B_2/dr^2	1230	1030	/
$2\nu_r + \nu_z = 8$	d^2B_8/dr^2	/	1730	1790
$3\nu_r = 7$	d^2B_7/dr^2	1150	1160	1170
$3\nu_r = 8$	d^2B_8/dr^2	1400	1410	1420
$3\nu_r = 10$	d^2B_{10}/dr^2	2000	/	1960

To maintain the isochronism, the concept of Integer Resonance Suppressor (IRS) [15] is adopted in Scheme 3. The working path of Scheme 3 crosses the $\nu_r = 3$, and with the help of IRS, the radial beam envelope can be inhibited. In addition, Scheme 3 crosses Walkinshaw resonance when the beam is almost extracted. Since energy gain per turn is relatively large, it can be verified by numerical simulation that the beam envelope grows only slightly when the amount of off-center is about 1 cm, and half envelop increases to 10 mm at the case of 3 cm off-center, which is shown in Fig. 4.

High order resonance $2\nu_r + 2\nu_z = 10$ is also under consideration. It is an inherent resonance in our machine, while the highest of magnetic field is 3rd, only small amount of driving term at extraction. A case of 0.5 Gs/m³ is simulated, and the phase of the B_{10} field is random. Figure 4 shows that the beam envelope is growing a little due to this resonance.

Various Solutions for Extraction

The following two methods are under consideration to increase turn separation for a clean extraction. 1) Layout of long drift sections can add a large number of high-frequency cavities to maximize the energy gain; 2) Off-centering injection can produce precession at the extraction position, increasing the separation of the last turn, but integer resonance needs to be carefully considered.

Scheme 2 utilizes integer resonance for extraction, tunes the working path near the extraction area reasonably, and controls $\nu_r \approx 3$ resonance to drive radial oscillation. The isochronism is sacrificed, which leads to the stretch of beam phase width and energy dispersion increasing during extraction. The beam envelope grows during precession extraction, as shown in Fig. 5.

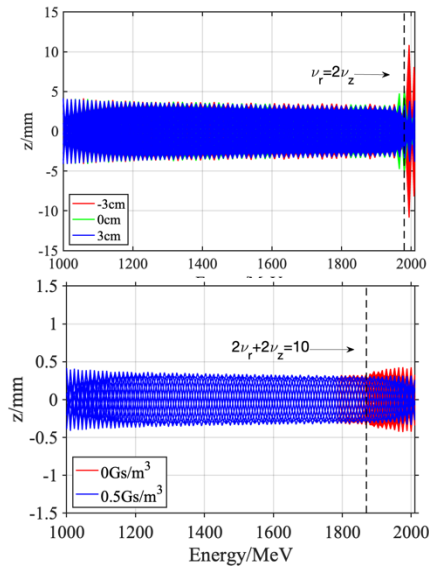


Figure 4: Vertical beam envelope of off-center beam, $\nu_r = 2\nu_z$ (up), $2\nu_r + 2\nu_z = 10$ (down).

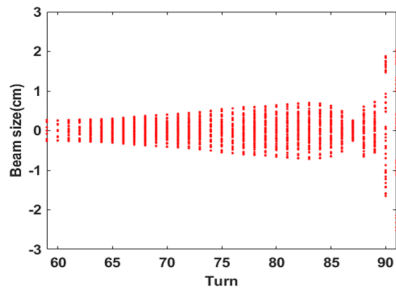


Figure 5: Radial beam envelope growth during precession extraction, scheme 2.

With the help of IRS and half-integer resonance extraction, the plan can be reconsidered in Scheme 3. Half-integer resonance extraction has a relatively mature solution in isochronous circular accelerators, and the turn separation is doubled to 25 mm, recording to Fig. 6.

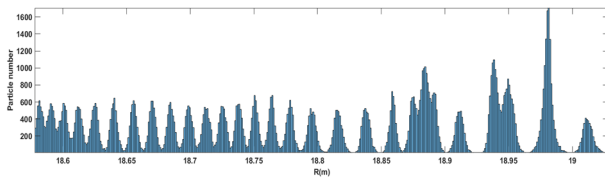


Figure 6: Particle distribution on radial probe.

Parallel Computing Results in the FFA machine

Some preliminary computation by OPAL-CYCL with AMR (adaptive mesh refinement) is undergoing in CIAE. Preliminary results with faster large-scale multi-particle simulation for Scheme 3 are presented below. The bunch's initial parameters for simulation are: transverse emittance is $2 \pi \text{mm} \cdot \text{mrad}$; phase width is 3° ; beam current is 3 mA/6 mA. Moreover, the transverse size of the bunch decreases to around $\pm 7 \text{mm}$ at the final turn, making it potentially appropriate for extraction. The followings are the

compared results with and without the space charge effect in more detail. As compared in the first and second rows of Fig. 7, the beam quality is significantly better without a space charge, demonstrating that the space charge effect is primarily responsible for the vortex effect in the CW FFA. It is also indicated in the second row and the third row in Fig. 7 that higher beam current results in a more significant space charge effect, which increases the transverse size near $\pm 1 \text{cm}$. Nevertheless, with higher energy gain provided by RF cavities and properly arranged extraction elements, turn separation is promisingly increased to 30 mm, which is suitable for extraction.

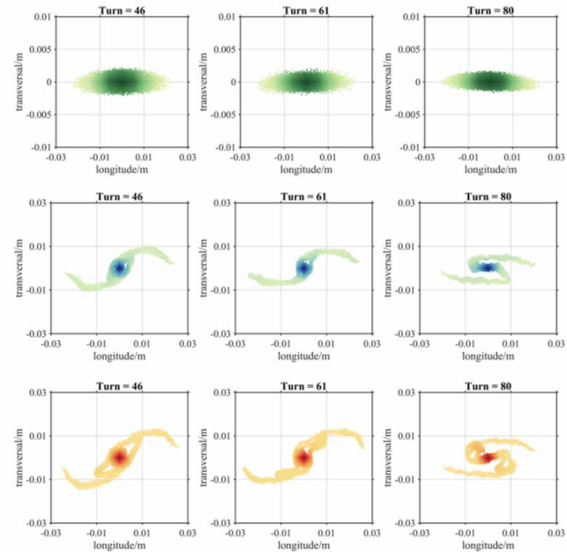


Figure 7: Longitudinal and transverse beam shape variation, from the 1st column to the 3rd column, 46, 61, 80 turns; from the 1st row to the 3rd row: 0 mA with space charge (green); 3 mA with space charge (blue-green); 6 mA with space charge (yellow).

RECENT PROGRESS IN KEY TECHNOLOGIES

Design and Verification of HTS Magnet System

Three different field maps are found for High-temperature superconducting (HTS), gap shaped magnet design. Full-scaled magnets are designed based on the FEM code. For the application of HTS in the 2 GeV FFA accelerator, third-order magnetic field matching, fringe field, and shielding current field are three major difficulties that need technological verification. An integral equation method has been developed to design gap-shaped magnets better. According to this method, final FEM models and magnetic field differences are shown in Fig. 8, which illustrates that the relative error of the mean-field can be adjusted to 2%.

Besides the theoretical analysis of full-scaled magnets, a scaled model of HTS magnets is also designed and fabricated at CIAE. The quarter scaled model is wound along the spiral angle of a full-scaled model to ensure the stress between turns is equals. Unlike LTS coils, this HTS mag-

Content from this work may be used under the terms of the CC-BY-4.0 licence (© 2022). Any distribution of this work must maintain attribution to the author(s), title of the work, publisher, and DOI

net is spineless and challenging to fit the spiral angle exactly. A 3-dimensional winding machine has been developed for this type of concave coil. But in practice, we adopted f-clamps instead to avoid customization and for rapid manufacturing.

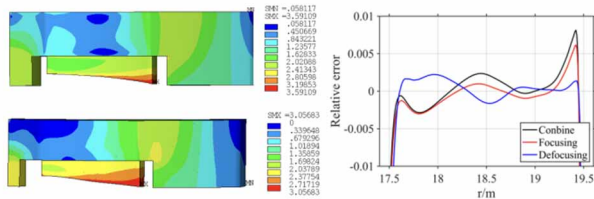


Figure 8: Magnetic field distribution map and relative deviation for the mean field.

The pancake coils and assembly are shown in Fig. 9. Since these HTS coils are no-insulated, each of the six double-pancakes will be tested in liquid nitrogen to check the insulative between turns after it has been wound. The time constant is calculated to ensure the consistency of these six double-pancakes. The HTS magnet assembly has completed the excitation test without an iron yoke. Field measurement results at 30 K show that the magnet can operate normally under the design's current value, which lays a solid foundation for the subsequent design of full-scale magnets.

As mentioned above, superconducting coils have been independently tested, and the experimental results of 6 sets of double-pancake coils show that they can work stably above 130 A. The combined coil assembly can be cooled to 25 K by cold helium gas and can run stably at the design current value of 270 A. At the same time, there is an adjustable range of 30 A. In other words, the coil assembly can be remapped to 300 A in 30 K, indicating that the winding technology of concave coils is successful and performable.

Moreover, the terminal voltage of HTS coils has been kept below 3 mV during the stability test in Fig. 10, which proves that this type of HTS magnet could be reliable in the future for FFA applications. In addition, we are planning to carry out radiative tests for this scaled magnet since the beam loss in the extraction region is inevitable, which will cause a quench of superconducting magnets.



Figure 9: Schematic diagram of the installation process of the 1:4 scaled magnet and the assembly.

A 1:4 scaled gap shaped iron is also designed and fabricated, which weighs approximately 7 tons. The field distribution of the theoretical design determines the shape of the gap. A spacer is located at the head of the iron to control the shape of the deformation. Mechanical analysis indicates that the amount of deformation is about 0.07 mm, and the field deviation is at the Gs level. The field distribution is measured and compared with the analytical result. Recently, HTS coils have been assembled with gap-shaped iron magnets to prepare for excitation and field measurement, as shown in Fig. 11. Excitation is carried out for this HTS magnet assembly, and the magnet is successfully ramping to 243 A at 25 K.

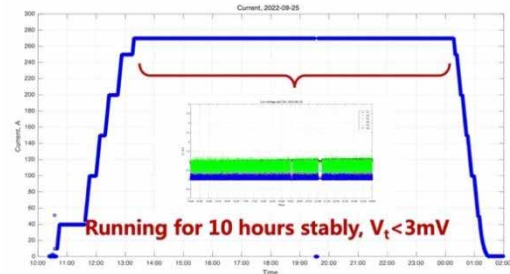


Figure 10: Terminal voltage of the whole HTS coil during stability test.



Figure 11: 1:4 scaled magnet assembly.

High Energy Efficiency RF system

For the 2 GeV FFA, N.C. (Normal Conducting) RF cavities will be applied to boost the proton beam energy from 800 MeV to 2 GeV. Due to the heavy beam loading, the development of the N.C. high-power waveguide type RF cavity with high-quality factor Q and high shunt impedance R is crucial. This would certainly be beneficial for the RF energy efficiency enhancement. Four geometries (i.e., the rectangular, the omega, the racetrack, and the boat ones) of the waveguide-type RF cavities were investigated extensively, and it is found that the boat shape RF cavity has the highest Q (~90000), and the highest R (11~20 MΩ along the radial beam aperture), and is the best candidate [16].

As the beam dynamics requirement, the high energy efficiency RF system of the 2 GeV FFA was designed to consist of 10/15 sets of identical sub-systems, as shown in Fig. 12.

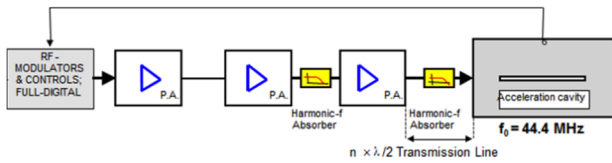


Figure 12: One typical sub-system of the high energy efficiency RF system

The final stage RF power amplifier was designed to provide RF input of up to 1.5 MW for each cavity. The 15 cavities are driven separately, thus, the RF amplitude is independently regulated while the phase of each cavity is locked with the master oscillator. Therefore, 15 MeV energy gain per turn can be obtained with an estimated consumption of about 1 MW power.

R&D studies on a 177.6 MHz 1:4 scale boat shape prototype cavity ($L \times W \times H = 2.4 \text{ m} \times 1.4 \text{ m} \times 2.5 \text{ m}$ for the copper cavity and the stainless-steel supports, while $L \times W \times H = 2 \text{ m} \times 0.5 \text{ m} \times 0.8 \text{ m}$ for the copper cavity only) were carried out, to investigate technical aspects of the RF cavity. The cavity's Q and R_{max} were calculated to be ~ 43500 and $\sim 7.61 \text{ M}\Omega$, respectively.

For the prototype cavity, $\sim 100 \text{ kW}$ designed RF power dissipated on the cavity walls is planned to be brought away by the cooling water, and a $\sim \pm 170 \text{ kHz}$ tuning range is demanded by deforming the RF cavity walls with the electric cylinders. With 35°C cooling water, the maximum temperature rise is $\sim 42^\circ\text{C}$ and is located at the left and right ends of the nose cones. To improve the mechanical design, a self-consistent multi-physics coupled simulation study (i.e., RF-thermal-structural-RF analysis) with ANSYS HFSS and Workbench [17] was carried out by using the mechanical model shown in Fig. 13, which includes ~ 280 body components. Figure 14 shows the ANSYS Project Schematic giving the data linkage between the Geometry, the HFSS Design, the Static-State Thermal, and the Static Structural.

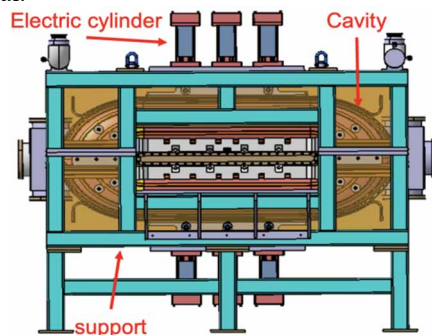


Figure 13: The mechanical model used in the multi-physics coupled simulation study.

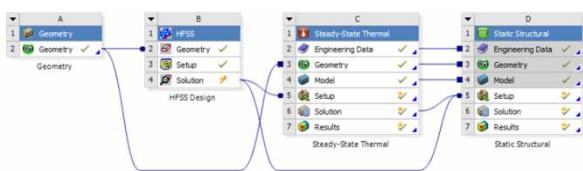


Figure 14: The ANSYS Project Schematic.

Considering the irregular shape of the boat-shaped RF cavity, it is very important to control the deformation during manufacturing and accurately determine the position during the welding. Special tooling and welding process were designed for manufacturing the cavity. Especially, Electron beam welding (EBW) technology was fully adopted to weld all the copper cavity walls together. Most of the parts of the copper cavity were formed by mold pressing. Due to the existence of the spring-back phenomena and the difficulty of finding an accurate reference for the wire-electrode cutting, additional CNC machining was applied. Finally, all the dimension errors were compensated by fine-finishing the nosecone according to the measurement during the cavity pre-assembly process. All of the water-cooling pipes were attached to the outer cavity wall by soldering. The Q and resonant frequencies were checked frequently to ensure the cavity's performance was consistent with the physical design.

Figure 15 shows one of the two half-cavities after the all-manual polishing and the surface roughness measurement, which is better than $0.1 \mu\text{m}$. After the quarter-scale cavity assembly was connected with the vacuum pump, the measured resonant frequency is $\sim 177.77 \text{ MHz}$ at a vacuum level of $\sim 1 \times 10^{-5} \text{ Pa}$. With maximum deformations of $\pm 2.5 \text{ mm}$ at both the upper and lower sides of the cavity body, the measured frequency tuning range is about $\pm 180 \text{ kHz}$. The measured unloaded Q is higher than 42300, which is $\sim 97\%$ of the calculated values of 43500. Figure 16 shows the onsite installation of the quarter-scale cavity at CIAE. The high-power test is being planned and will be conducted very soon.



Figure 15: One of the two half-cavities and the surface roughness measurement.



Figure 16: The onsite installation of the quarter-scale cavity at CIAE.

Content from this work may be used under the terms of the CC-BY-4.0 licence (© 2022). Any distribution of this work must maintain attribution to the author(s), title of the work, publisher, and DOI

CONCLUSION

Due to its diverse application, the high energy and high current isochronous proton accelerator are actively researched in the modern accelerator field. Based on the extensive experience of successful construction, commissioning, and operation of the high-power compact cyclotron CYCIAE-100, a CW FFA is proposed by CIAE to produce a 2 GeV/6 MW proton beam. Beam dynamics results show good isochronism towards 2 GeV and have a very large acceptance of the beam phase space. Resonance analysis shows the beam quality could be guaranteed because of the flexible modulating of the tune diagram by precisely adjusting the magnetic field gradient in a wide radial range. The turn separation can be increased to ~3 cm with 5 additional cavities and off-centered injection, which seems to be enough for 6 MW beam extraction. R&D Activities for key components, including the 1:4 HTS magnet and the high energy efficiency RF system, are finished for the 2 GeV high power CW FFA accelerator complex.

ACKNOWLEDGMENTS

We would like to extend our cordial gratitude to experts from TRIUMF, PSI, INFN-LNS, and the international cyclotron community for their long-term support and the recent email discussion with Dr. Baartman and Dr. Calabretta about the beam physics for the 2 GeV machine. The authors would also like to thank Dr. Jianjun Yang for the valuable discussion in person and Dr. Ming Li and Dr. Tianjian Bian for their previous research, which are cited in the reference list.

REFERENCES

- [1] R. Garoby *et al.*, “Proton drivers for neutrino beams and other high intensity applications”, *J. Phys. Conf. Ser.*, vol. 408, no. 1, Feb. 2013, pp. 012016.
doi:10.1088/1742-6596/408/1/012016
- [2] C. L. Morris *et al.*, “New Developments in Proton Radiography at the Los Alamos Neutron Science Center (LANSCE)”, *Exp. Mech.*, vol. 56, pp. 111-120, 2016.
doi:10.1007/s11340-015-0077-2
- [3] C. Rubbia *et al.*, “Conceptual design of a fast neutron operated a high power energy amplifier”, CERN/AT/95-44 (ET).
- [4] Th. Stammbach, “High Intensity Problems, Revisited or Cyclotron Operation Beyond Limits”, in *Proc. Cyclotrons '98*, Caen, France, Jun 1998, paper E-01, pp 369-376.

- [5] A. Jansson, “The Status of the ESS Project”, in *Proc. IPAC'22*, Bangkok, Thailand, Jun. 2022, pp. 792-795.
doi:10.18429/JACoW-IPAC2022-TUIYGD1
- [6] Luciano Calabretta *et al.*, “Cyclotrons and FFAG Accelerators as Drivers for ADS”, Internal Report, BNL-111770-2016-JA, 2016.
- [7] Y. Ishi *et al.*, “Status report on KURNS FFAG Facility”, FFAG-18 Workshop, Sep. 2018.
- [8] T. J. Zhang *et al.*, “A New Solution for Cost Effective, High Average Power (2 GeV, 6 MW) Proton Accelerator and its R&D Activities”, in *Proc. Cyclotrons'19*, Cape Town, South Africa, Sep. 2019, pp. 334-339.
doi:10.18429/JACoW-CYCLOTRONS2019-FRA01
- [9] M. Seidel *et al.*, “Production of a 1.3 MW Proton Beam at PSI”, in *Proc. IPAC'10*, Kyoto, Japan, May 2010, paper TUYRA03, pp. 1309-1313.
- [10] R. A. Baartman, “Space Charge Limit in Separated Turn Cyclotrons”, in *Proc. Cyclotrons'13*, Vancouver, Canada, Sep. 2013, paper WE2PB01, pp. 305-309.
- [11] L. Laslett *et al.*, “On intensity limitations imposed by transverse space-charge effects in circular particle accelerators”, Summer Study on Storage Rings, BNL Report 7534, pp. 325-367, 1963.
- [12] R. A. Baartman, “Intensity Limitations in Compact H⁻ Cyclotrons”, in *Proc. Cyclotron '95*, Cape Town, South Africa, Oct. 1995, pp. 440-445.
- [13] V. P. Yakovlev *et al.*, “The Energy Efficiency of High Intensity Proton Driver Concepts”, in *Proc. IPAC'17*, Copenhagen, Denmark, May 2017, pp. 4842-4847.
doi:10.18429/JACoW-IPAC2017-FRXCBB1
- [14] T. Zhang *et al.*, “Innovative research and development activities on high energy and high current isochronous proton accelerator”, *ICFA Beam Dynamics Newsletter*, vol. 84, JINST_212P_1022, to be published.
- [15] T. Bian *et al.*, “Possible solution for the integer resonance crossing problem of GeV-class isochronous fixed-field alternating gradient accelerators”, *Nucl. Instrum. Methods*, vol. 1031, pp. 166594, May 2022.
<https://doi.org/10.1016/j.nima.2022.166594>
- [16] S. Pei *et al.*, “Design on High Quality Factor and High Shunt Impedance Waveguide-type RF Cavity for 2 GeV FFAG Proton Accelerator”, *Atomic Energy Sci. Technol.*, vol. 54, no. 8, 2020, pp. 1519-1524.
doi:10.7538/yzk.2019.youxian.0495
- [17] ANSYS is a finite element code developed by ANSYS Inc. Canonsburg, PA, <https://www.ansys.com/>